JACS
JOURNAL OF THE AMERICAN CHEMICAL SOCIETY
Article
pubs.acs.org/JACS

Optimizing Electron Transfer Mediators Based on Arylimidazoles by Ring Fusion: Synthesis, Electrochemistry, and Computational Analysis of 2-Aryl-1-methylphenanthro[9,10-*d*]imidazoles

Robert Francke and R. Daniel Little*

Department of Chemistry and Biochemistry, University of California, Santa Barbara, California 93106-9510, United States

Supporting Information

ABSTRACT: A significant improvement of the properties of redox catalysts based on the triarylimidazole framework can be achieved with a simple structural modification. By linking the *ortho*-carbons of the aromatics positioned at C-4 and C-5, a fused framework is generated, removing the distortion from planarity and enhancing the influence of the substituents on the redox properties. This modification leads not only to a much broader range of available redox potentials for the resulting phenanthro[9,10-*d*]imidazoles but also to improved stability of the corresponding radical cation. These concepts were verified with eight new phenanthro[9,10-*d*]imidazole derivatives, using cyclic voltammetry and DFT calculations. For this purpose, an optimized and general synthetic route to the desired compounds was developed. An excellent linear correlation of the calculated effective ionization potentials with the experimental oxidation potentials was obtained, allowing for an accurate prediction of oxidation potentials of derivatives yet to be synthesized. Moreover, high catalytic activity was found for electro-oxidative C−H activation reactions.

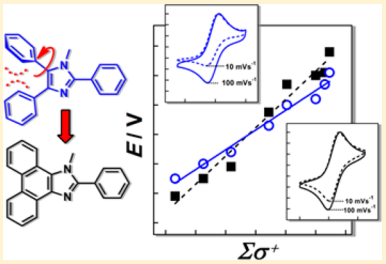

INTRODUCTION

Organic electrosynthesis is recognized as an environmentally compatible methodology since toxic and dangerous oxidizing or reducing reagents can be replaced and the overall energy consumption can be reduced.[1,2] Moreover, unstable or hazardous reagents can be produced in situ and reactions carried out under very mild conditions.[3−5] One approach to increase the efficiency of electro-organic synthesis is to use electrochemically generated redox agents. Since the electron transfer step is shifted from a heterogeneous to a homogeneous process (an indirect electrolysis), the kinetic inhibition which is usually associated with the electron transfer from electrode to substrate can be eliminated. Typically, higher and/or totally different selectivity is achieved.[6−8] If one or more of the subsequent steps is an irreversible chemical reaction, then the electron transfer can occur even against a potential gradient.[8,9] Therefore, much higher or totally different selectivity can be achieved with lower energy consumption. In some difficult cases, electron transfer mediators help to avoid overoxidation of the substrate or avoid electrode passivation that may result by the formation of a polymer film on the electrode surface.[8,10] Ideally, the mediator engages in a reversible redox couple, one that is initiated at the electrode and is followed by a reaction of interest, thereby allowing for catalytic employment of the electron transfer mediator, in order to avoid reagent waste and difficult separation procedures.

Over the past decade, many intriguing new developments have been observed in this field, including indirect flash electrochemistry, mediated reductive dehalogenation using *o*-carboranes, or housane rearrangements triggered by redox catalysis.[11−16] Furthermore, compounds originally designed for electron transfer mediation currently attract attention in other fields. For instance, given the similarities between photosensitized and electrochemically mediated transformations, it is reasonable to anticipate that catalysts originally designed for indirect electrosynthesis will likely prove useful as excited state electron transfer agents in photoinitiated processes.[17] Another application of such compounds lies in the field of battery research, where they have been used as redox shuttles for overcharge protection.[18]

The most popular oxidative mediator system is represented by the triarylamines, with numerous applications and a broad range of accessible potentials.[10,15,16,19−24] However, they tend to undergo intermolecular oxidative coupling reactions, thereby reducing the reversibility of the redox couple and making a *para* substitution of the aryl rings necessary.[25,26] Another drawback to their use in some instances is that a high molar percentage of the triarylamine must be employed in order to achieve a complete conversion.[10,16] To circumvent many of these issues, we recently developed a new class of metal-free, easy to synthesize redox catalysts based on the triarylimidazole framework (**1**) (see Scheme 1, left).[27] We have demonstrated that their oxidation potential can be tuned within a wide range by modification of the substitution pattern on the aromatics.[28] They have already proven to be useful mediators for the activation of benzylic C−H bonds under mild conditions (see Scheme 1, right). While the range of accessible potentials for triarylimidazoles is good, their significant distortion from planarity presents a problem because the effectiveness of

Received: October 23, 2013
Published: December 13, 2013

dx.doi.org/10.1021/ja410865z | *J. Am. Chem. Soc.* 2014, 136, 427−435

Scheme 1. Triarylimidazoles (1) and Phenanthro[9,10-*d*]imidazoles (2) as Mediators for Electro-organic Synthesis (Left) and Application for Electro-oxidative C−H Activation at Benzylic Positions (Right)

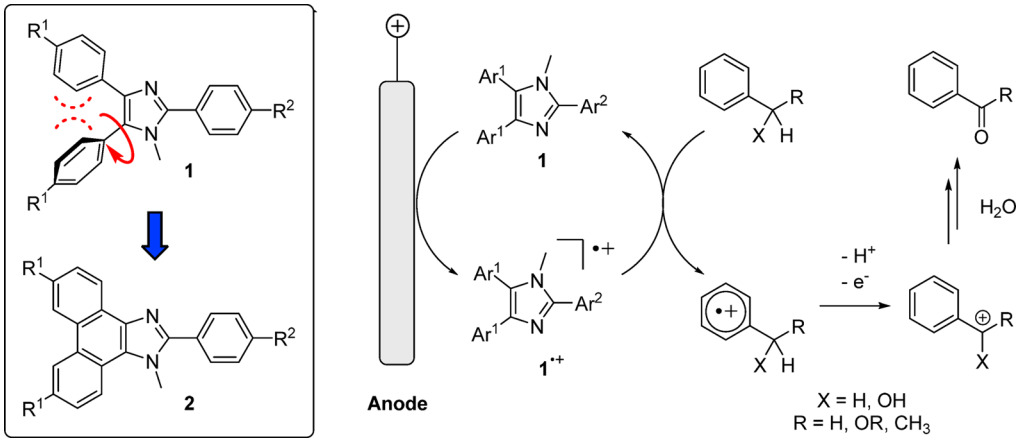

Table 1. Substitution Patterns, Sum of the σ^+ Values, and Oxidation Potentials $E_{ox,1}$ (vs $Ag/AgNO_3$) of the Synthesized Phenanthroimidazoles 2 and the Corresponding Triarylimidazoles 1

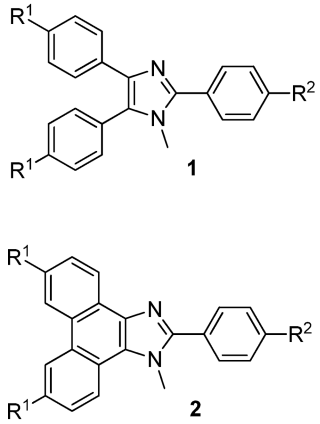

R^1	R^2	$\Sigma\sigma^+$	Triarylimidazoles 1		Phenanthroimidazoles 2	
			No.	$E_{ox,1}$ / V[28]	No.	$E_{ox,1}$ / V
Br	F	0.23	**1a**	1.01	**2a**	1.09
H	Br	0.15	**1b**	0.97	**2b**	1.01
H	H	0	**1c**	0.92	**2c**	1.00
Br	OMe	-0.48	**1d**	0.90	**2d**	0.97
H	OMe	-0.78	**1e**	0.83	**2e**	0.88
OMe	Br	-1.41	**1f**	0.74	**2f**	0.69
OMe	Me	-1.87	**1g**	0.70	**2g**	0.65
OMe	OMe	-2.34	**1h**	0.65	**2h**	0.59

substituents to influence the potential is impaired.[28] Moreover, the limited stability of the radical cation formed upon electro-oxidation leads to a quasi- rather than a fully reversible oxidation process.[27] In the present work, we demonstrate how these problems can be overcome by linkage of the *ortho*-carbons of the aromatics positioned at C-4 and C-5 of the imidazole subunit to generate the fused framework **2**. Toward this end, a series of substituted phenanthro[9,10-*d*]imidazoles was synthesized, an optimized and general procedure was developed, and their characteristics were studied using cyclic voltammetry and bulk electrolysis. Using DFT calculations, the redox properties of these systems could be explained and oxidation potentials of derivatives yet to be synthesized become predictable. We note with interest that our systems may be of use in the field of optoelectronics. This realization stems from recent reports that the photoemissive properties of phenanthro-[9,10-*d*]imidazoles combined with their high thermal stability and easy modifiability make them useful building blocks for the assembly of functional layers in organic light-emitting diodes (OLEDs) or for photosensitizers in dye-sensitized solar cells.[29−33]

RESULTS AND DISCUSSION

Synthesis. Eight 2-aryl-1-methylphenanthro[9,10-*d*]-imidazoles (**2**) bearing methoxy, methyl, bromo, and fluoro moieties in three different positions were synthesized (for particular substitution patterns, see Table 1).[34] Initially, we attempted a direct condensation of phenanthrene-9,10-quinone **3** with benzaldehyde **4**, methylamine, and ammonium acetate.[31,32] Unfortunately, the method primarily afforded a mixture of oxazoles and several structures where the imidazole ring failed to form.

In further attempts, **3**, **4**, NH_4OAc, and *N*-methylamine were allowed to react in the presence of NaH_2PO_4 in a manner analogous to a procedure that was previously used to synthesize 1-methyltriarylimidazoles, **1**.[37] Once again, however, mostly oxazole formation was observed. We then explored a two-step sequence calling first for the condensation of **3** and **4**, in the presence of 2 equiv of NH_4OAc, leading to the formation of the 1*H*-imidazole, followed by N-methylation. For the first step, we tried a procedure known to lead to unsubstituted 2-aryl-1*H*-phenanthro[9,10-*d*]imidazoles.[38] Although this approach turned out to be more successful in terms of imidazole ring formation, the 1*H*-imidazole was accompanied by substantial amounts of side products, thereby leading to a tedious

dx.doi.org/10.1021/ja410865z | J. Am. Chem. Soc. 2014, 136, 427−435

Scheme 2. Synthesis of Substituted Phenanthro[9,10-*d*]imidazoles 2

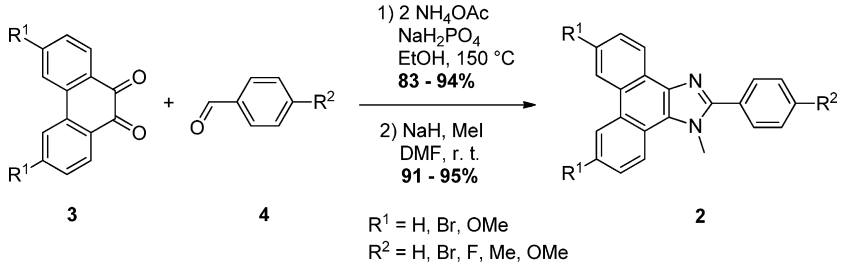

Scheme 3. Synthesis of Substituted Phenanthrene-9,10-quinones as Precursors for Phenanthro[9,10-*d*]imidazoles 2[35,36]

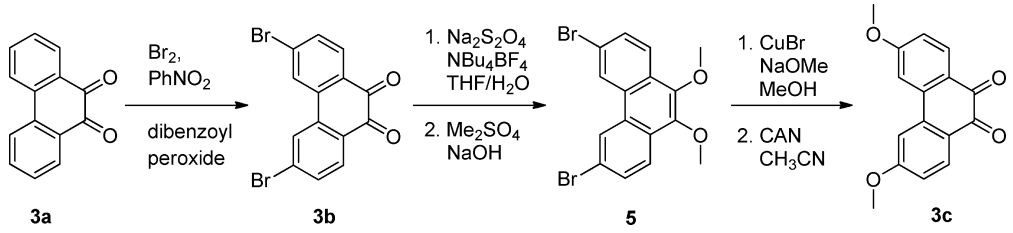

purification process. We eventually discovered that a clean conversion to the 1*H*-imidazole framework could be achieved in the presence of NaH_2PO_4 with ethanol as solvent at 150 °C (sealed tube; see Scheme 2), rendering pure 1*H*-phenanthroimidazoles in 83−94% yield after simple trituration of the crude product. The subsequent N-methylation proceeds smoothly at room temperature in DMF after deprotonation of the 1*H*-imidazole with NaH and addition of methyl iodide (yield after recrystallization = 91−95%).[39]

Bromo- and methoxy-substituted phenanthrene-9,10-quinones **3b** and **3c** were obtained using a sequence elaborated by MacLachlan et al. (see Scheme 3),[35] starting with the bromination of **3a** using Br_2 in nitrobenzene and dibenzoyl peroxide as a radical initiator.[36] Since a direct methoxylation of **3b** failed,[35] it was first reduced and then converted to the bisenol ether **5** prior to aryl methoxylation with NaOMe in the presence of catalytic amounts of CuBr. The resulting intermediate, 3,6,9,10-tetramethoxyphenanthrene, was then oxidized using ceric ammonium nitrate to obtain phenanthroimidazole precursor **3c**.

Electrochemical Characterization. The electrochemical properties of compounds **2** were studied with cyclic voltammetry, using an electrolyte consisting of 0.2 M $LiClO_4$ in CH_3CN/CH_2Cl_2 (4:1 by volume), a glassy carbon working electrode, and a platinum wire as the counter electrode. A silver wire in 0.01 M $AgNO_3$, separated from the analyte by a Vycor frit, was used as the reference. To allow comparison of the potentials recorded herein with other common reference electrodes, one simply adds +87 mV to convert to the ferrocene redox couple, +298 mV for SCE and +542 mV for NHE.[40] Each of the phenanthroimidazoles exhibited between two and four peaks in the anodic scan and no activity in the negative potential range (see Supporting Information Table S1). At 100 mV s^{-1}, the first redox couple is chemically and electrochemically reversible ($\Delta E_p \approx 60$ mV indicative of electrochemical reversibility, and $i_{p,ox}/i_{p,red} \approx 1$ demonstrating chemical reversibility), indicating that the heterogeneous electron transfer is fast and that the species formed during the oxidation process is stable on the voltammetry time scale.[41] Since the peak separation ΔE_p between anodic and cathodic peaks points toward a single electron transfer, it can be assumed that the oxidized species is radical cation $\mathbf{2}^{\bullet+}$. Its role in electrocatalytic processes is discussed later and is supported by computational results.

Since the potential difference between the first and the second oxidation peak ($E_{ox,1}$ and $E_{ox,2}$) is between 350 and 480 mV, depending on the derivative (see Supporting Information Table S1 and Figures S3−S5), $\mathbf{2}^{\bullet+}$ can be formed exclusively by operating at the less positive potential. Presumably, the second irreversible oxidation peak corresponds to the oxidation of $\mathbf{2}^{\bullet+}$ to dication $\mathbf{2}^{2+}$. This dication seems to undergo a fast chemical reaction (probably deprotonation), and the following peaks could correspond to the oxidation of the products of the follow-up reaction(s). A large difference between the potentials $E_{ox,1}$ and $E_{ox,2}$ is essential for application in electrosynthesis in order to avoid side reactions and loss of catalytic activity. Another important attribute of the systems described herein is that they are electrochemically inert in the negative potential range, out to the negative stability limit of the electrolyte (−2.4 V vs Ag/$AgNO_3$). The practical implication of this observation is that an undivided electrolysis cell may be considered for possible applications, as long as the chemical follow-up reaction is fast enough to avoid diffusion of $\mathbf{2}^{\bullet+}$ to the cathode where it would be discharged.

The first oxidation peak potentials of **2** ($E_{ox,1}$) are summarized in Table 1 and compared to the corresponding triarylimidazoles **1**.[28] A full list of all peak potentials is provided in the Supporting Information (see Table S1). The values are in the range between 0.59 V (**2h**, R^1 = OMe, R^2 = OMe) and 1.09 V (**2a**, R^1 = Br, R^2 = F) versus Ag/$AgNO_3$ (0.89−1.39 V vs SCE and 1.13−1.63 vs NHE). With such relatively high oxidation potentials, $\mathbf{2}^{\bullet+}$ can be considered to be strong oxidizing agents, situated in the same range of common oxidizers such as Ce^{3+}/Ce^{4+} (1.61 V vs NHE) or the tris-*para*-bromophenylamine radical cation (1.30 V vs NHE).[8] The potentials follow a clear trend with the values increasing as the number of electron-withdrawing substituents (Br, F) increases and the number of electron-donating substituents (OMe, Me) diminishes. With the compounds synthesized thus far, a potential range of 0.5 V is accessible, which means an increase of about 40% compared to the equally substituted triarylimidazoles **1** (potential range for **1**: 0.36 V). The influence of the

dx.doi.org/10.1021/ja410865z | J. Am. Chem. Soc. 2014, 136, 427−435

substituents on the electronic character of the aromatic ring system is therefore significantly enhanced.

As previously noted, an important characteristic of an electron transfer mediator is the reversibility of its redox couple. Low reversibility usually means that the mediator is prone to side reactions, leading to lower catalytic turnover numbers. As noted above, the first redox process for **2** is reversible at a scan rate of 100 mV s^{-1}. Furthermore, the ratio between the anodic and cathodic peak current is not significantly affected by the substitution pattern (see Figure S1). In order to compare the reversibility of systems **2** and **1**, the voltammograms were recorded at a lower scan rate; the results for **1e** and **2e** are plotted in Figure 1 (R^1 = H, R^2 =

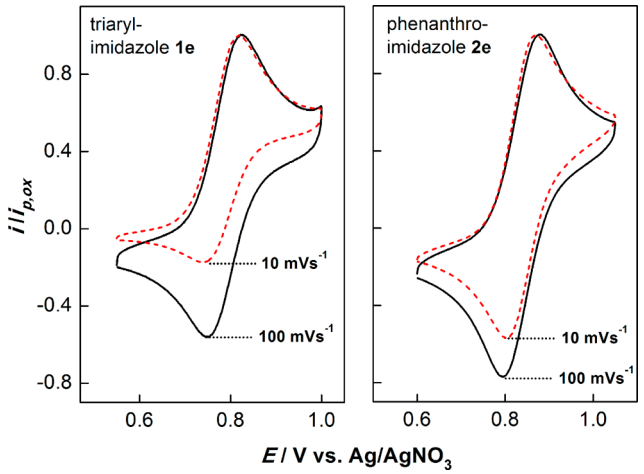

Figure 1. Cyclic voltammograms of compounds **1e** (left) and **2e** (right). Scan rate: 100 mV s^{-1} (solid line) and 10 mV s^{-1} (dashed line).

OMe; for additional examples, see Figure S2). For ease of comparison, the observed current is normalized to the peak current $i_{p,ox}$; thus the ordinate is illustrated as $i/i_{p,ox}$. Whereas at 10 mV s^{-1} for **1e** the current drops substantially during the back-scan, only a slight decrease of the cathodic current is visible for **2e**. These results impressively demonstrate how much more stabilized the fused framework $\mathbf{2}^{\bullet+}$ is compared to $\mathbf{1}^{\bullet+}$. Compared to the triarylamines, for which quasi-reversibility can only be achieved by blocking each of the *para*-positions on the aryl rings,[23,26] the stability of the radical cation $\mathbf{2}^{\bullet+}$ is even more pronounced. Oxidative couplings do not seem to play an important role since reversibility is achieved with partially blocked derivatives **2b** and **2e** as well as with unsubstituted compound **2c**. It should be noted that phenanthroimidazoles without N-substitution undergo an irreversible oxidation process (see Figure S6), most likely due to deprotonation after formation of the radical cation. Hence, N-alkylation seems to be crucial for application as an electrocatalyst.

Computational Analysis and Empirical Correlations. As noted earlier, the potential range accessible to compounds **2a**−**2h** is 0.5 V. Compared to the identically substituted triarylimidazoles **1a**−**1h** whose range is 360 mV, this amounts to an increase of about 40%. A mathematical description of the influence of the substituents on the oxidation potential $E_{ox,1}$ was obtained by plotting the observed $E_{ox,1}$ versus the sum of the Hammett σ^+ constants of the substituents appended to the aryl rings.[42,43] The slope provides a measure of the influence of the substituents upon the observed potential, while the intercept refers to the oxidation potential of the unsubstituted compound of the series.[43,44] For both systems **1** and **2**, a linear relationship is observed (see Figure 2), with a coefficient of determination (R^2) of 0.963 for **2** (see eq 1) and 0.973 for **1** (see eq 2).

$$E_{ox,1}(\mathbf{2}) = 1.015 + 0.192 \sum \sigma^+ \quad (R^2 = 0.963) \tag{1}$$

$$E_{ox,1}(\mathbf{1}) = 0.949 + 0.134 \sum \sigma^+ \quad (R^2 = 0.973) \tag{2}$$

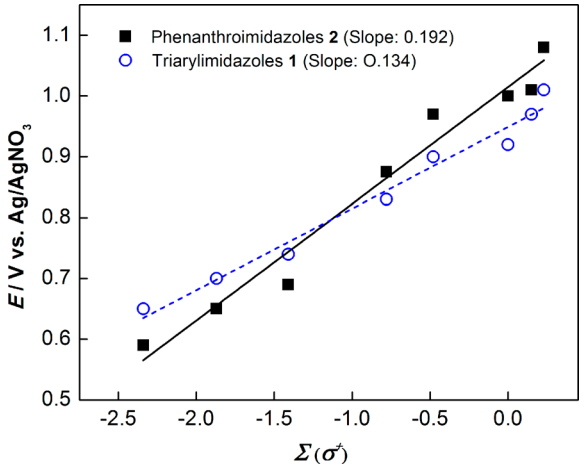

Figure 2. Plot of the observed oxidation potential $E_{ox,1}$ versus the sum of Hammett σ^+ values, $\Sigma\sigma^+$.

Thus, in both cases, the correlation of $E_{ox,1}$ with $\Sigma\sigma^+$ provides a convenient way to estimate the oxidation potential of a compound not yet synthesized. Furthermore, we note that a comparison of the slopes for the triarylimidazole framework **1** with that of the phenanthroimidazole structures **2** reveals that the influence of the substitution pattern is much more pronounced for the latter because the slope increases by 43%, from 0.134 to 0.192.

A reasonable explanation of the considerably higher Hammett slope is revealed when one considers the dihedral angles (ϕ, ϕ', and ϕ'', see Figure 3, top) of the computed structures of the unsubstituted systems **1c** and **2c** (Figure 3, second row from top). Each dihedral reflects the degree to which the aromatic rings deviate from the planarity of the imidazole core. The geometry-optimized structures were obtained using the B3LYP hybrid functional together with the 6-31+G* basis set.[45] Solvation effects were accounted for using the polarized continuum model SMD with acetonitrile as solvent.[46] The largest torsion in framework **1** is expected for ϕ since the aryl group appended to C-5 is adjacent to a second aryl moiety and a methyl group. Indeed, for **1c**, a very significant twist of the aryl ring out of the plane is observed (ϕ = 58°). In comparison, the distortion for the phenanthro-imidazole **2c** at the equivalent location is very small (ϕ = 3°). Also, for **1c**, the aryl rings positioned at C-4 and C-2 exhibit strong torsions with ϕ' = 34° and ϕ'' = 40°. In contrast, for **2c**, the dihedral angle is slightly larger at position 2 (ϕ'' = 45°), while dihedral angle ϕ' is 0.

Obviously, the sum of the dihedral angles is significantly smaller for **2** than for **1**. This implies that there should be increased delocalization with a concomitant improvement in the ability of substituents to communicate their electronic character. Consequently, each substituent that can interact with the π-system by resonance should have a greater influence on

dx.doi.org/10.1021/ja410865z | J. Am. Chem. Soc. 2014, 136, 427−435

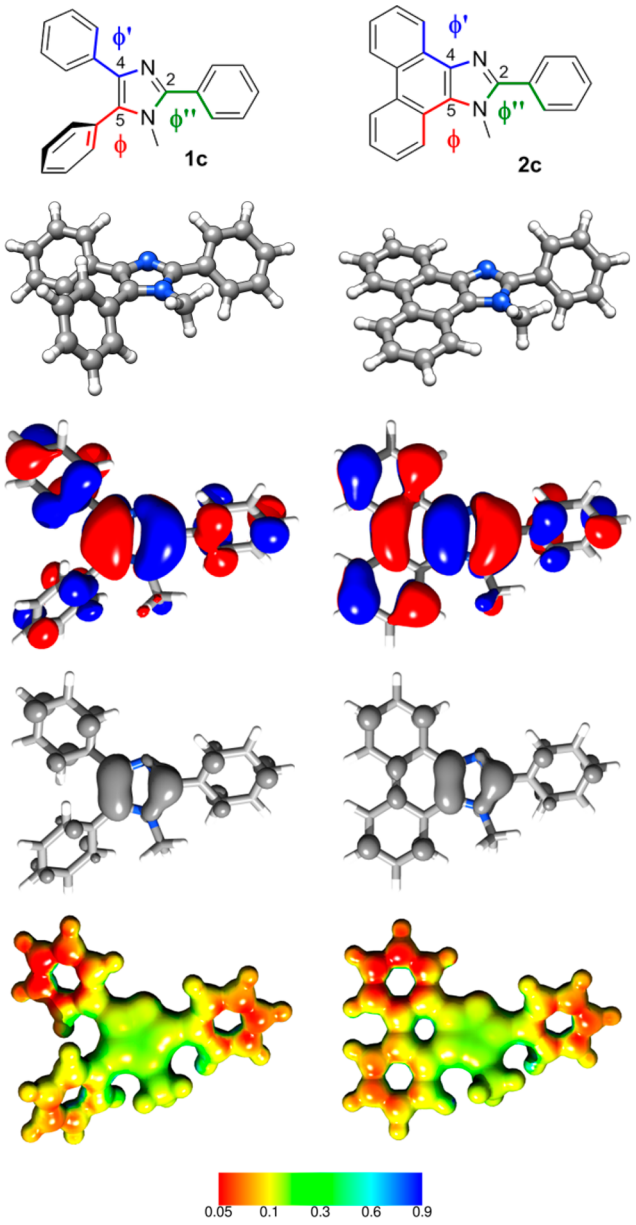

Figure 3. Dihedral angles ϕ, ϕ', and ϕ'' of **1c** and **2c** (top); computed geometries (second row from top) and HOMO maps (third row from top) for **1c** (left) and **2c** (right); spin density (fourth row from top) and electrostatic potential (bottom row; unit for color definition: kcal mol^{-1} e^{-1}) for radical cations $\mathbf{1c}^{\bullet+}$ (left) and $\mathbf{2c}^{\bullet+}$ (right); structures and surfaces calculated on the B3LYP/6-31+G* level (solvent: acetonitrile).

the oxidation potential in the phenanthroimidazoles **2**. As noted in Figure 3 (third row from top), the HOMO of **2** is spread throughout the phenanthro and imidazole subunits, and the aryl ring appended to C-5 in **2c** contributes more significantly than the analogous ring in **1c**.

In the computed structures of the corresponding radical cations $\mathbf{2c}^{\bullet+}$ and $\mathbf{1c}^{\bullet+}$, the dihedral angles ϕ, ϕ', and ϕ'' alter significantly compared to their neutral forms. For $\mathbf{1c}^{\bullet+}$ each angle decreases between 5 and 10°, allowing for a better conjugation and therefore better stabilization of the radical and the positive charge. For **2c**, a slight increase of ϕ and ϕ' is observed, a shift from 3 to 5° and from 0 to 1°, respectively. Compared to the neutral form **2**, the aryl ring at C-2 twists into the plane with a decrease of ϕ'' from 45 to 33°. Again, the sum of the dihedral angles is significantly smaller for $\mathbf{2c}^{\bullet+}$, indicating that compared to $\mathbf{1c}^{\bullet+}$ an improved stabilization of the radical and the positive charge is achieved by ring fusion. This conclusion is consistent with the higher reversibility of the oxidation of **2** compared to **1** (see Figure 1). In order to confirm and generalize the results obtained for the unsubstituted systems **1c** and **2c**, the dihedral angles ϕ, ϕ', and ϕ'' for all computed compounds (**1a**−**1h**, $\mathbf{1a}^{\bullet+}$−$\mathbf{1h}^{\bullet+}$, **2a**−**2h**, and $\mathbf{2a}^{\bullet+}$−$\mathbf{2h}^{\bullet+}$) were determined and summarized in Table S7; in each case, the same trend is observed.

Apart from the increased Hammett slope and the improved reversibility, a further advantage inherent to the phenanthroimidazoles could arise from the planarity of the radical cation. In contrast to $\mathbf{1}^{\bullet+}$, the nearly flat radical cation $\mathbf{2}^{\bullet+}$ provides a more accessible platform especially when the substrate to be oxidized contains an aromatic electrophore that might engage in cation−π interactions.

Moreover, the computational results reveal that for both $\mathbf{2c}^{\bullet+}$ and $\mathbf{1c}^{\bullet+}$ the spin density (Figure 3, fourth row from top) and the positive charge (Figure 3, bottom row) are mainly located within the imidazole subunit. It can therefore be assumed that the imidazole ring represents the reactive center of the activated form of the mediator. Since this center is more exposed in $\mathbf{2c}^{\bullet+}$ than in $\mathbf{1c}^{\bullet+}$, we anticipate improved interaction between the SOMO (singly occupied molecular orbital) of the oxidized form of the mediator and the HOMO of the substrate. This notion that greater accessibility can be correlated with oxidizability has been examined by Kochi et al. for the photoinduced electron transfer reaction between excited state quinones and a series of arene donors.[47] Their study indicated how the electron transfer can be changed from an inner-sphere to an outer-sphere mechanism by controlling the steric periphery of the arene donors, thereby influencing the ability of the reacting partners to approach one another. Whether there is a similar influence of the planarity of a mediator system $\mathbf{2}/\mathbf{2}^{\bullet+}$ on the electron transfer rate remains to be explored.

Compounds **2a**−**h** were examined to determine whether there is an empirical relationship between the first oxidation potential $E_{ox,1}$ and the effective ionization potential I_P* (calculation method 1) or the HOMO energy ε_H (calculation method 2), and these quantities were determined using DFT-based methods. Should they exist, such correlations would provide a convenient tool that could be used to predict $E_{ox,1}$ for a structure yet to be synthesized and allow one to tailor a mediator to a specific redox reaction whose oxidation potential is known. We were also interested in determining the minimum level of theory necessary for an accurate prediction since the use of larger basis sets, diffuse orbitals, and the inclusion of solvent models increases computation times. For the calculation of the effective ionization potentials (I_P*), we used the B3LYP hybrid functional starting with a 6-31G* basis set (vacuum) followed by inclusion of diffuse functions (6-31+G*, vacuum). Finally, acetonitrile was incorporated because it was the solvent used in the CV experiments,[48] by applying the 6-31+G* basis set in combination with the polarized continuum model SMD.[46] The values for I_P* were obtained according to eq 3 by subtraction of the SCF energy ε_{SCF} of radical cation $\mathbf{2}^{\bullet+}$ from that of the neutral form **2** (see Tables S2−S4).

$$I_P^* = \varepsilon_{SCF}(\mathbf{2}^{\bullet+}) - \varepsilon_{SCF}(\mathbf{2}) \quad (3)$$

dx.doi.org/10.1021/ja410865z | J. Am. Chem. Soc. 2014, 136, 427−435

Both energies ε_{SCF} corresponded to the geometry-optimized structures. By adopting this approach, the differences in time scale between a voltammetry experiment and vertical excitation are taken into consideration. In particular, the radical cation has sufficient time to relax to an energy minimum due to the significantly longer voltammetry time scale. A similar analysis has been used by Fry et al. in conjunction with substituted benzalacetophenones and triarylamines.[43,44] Because this approach does not satisfy the definition of the ionization potential, we prefer to use the term effective ionization potential and use the symbol I_P*.

According to Koopman's theorem, the ionization potential I_P can be derived from the HOMO energy ε_H using the following relationship.[49]

$$I_p = -\varepsilon_H \quad (4)$$

In contrast to Hartree−Fock theory, this relationship becomes accurate when DFT-based methods are used to calculate ε_H.[50,51] These I_P values have a different physical significance than I_P* derived from the subtraction approach described above (vertical ionization potential vs energy difference between **2** and $\mathbf{2}^{\bullet+}$, eq 3). In this context, we calculated ε_H of **2** for each level of theory (see Table S5) to determine whether there is an empirical relationship between $E_{ox,1}$ and ε_H for this series of compounds (calculation method 2).

For both method 1 and method 2, a linear relationship is observed at each level of theory. In Table 2, the parameters for the linear regressions are summarized, and in Figure 4, the plots of $E_{ox,1}$ versus I_P* and $E_{ox,1}$ versus ε_H are depicted.[52] Excellent linear correlations with R^2 close to unity can be obtained applying method 1, using both B3LYP/6-31G* and B3LYP/6-31+G*, with slightly better results when the solvent model is applied. Apparently, inaccuracies are canceled out when the energy difference between the neutral form and radical cation is considered. Thus, the improvement obtained by using a more sophisticated computational method is rather small. All three outperform the Hammett approach using $\sum\sigma^+$ (see eq 1) though the simplicity of the latter is most appealing.

In contrast, with a coefficient of determination R^2 of 0.939, the employment of method 2 (B3LYP/6-31G*/vacuum) is rather imprecise. However, R^2 increases dramatically as the sophistication of the method increases; calculations using B3LYP with a 6-31+G* basis set and inclusion of solvent afforded an excellent linear correlation of $E_{ox,1}$ versus ε_H (with R^2 = 0.993). We conclude that choosing an appropriate level of theory seems to be essential when method 2 is used. The key to obtaining the highest accuracy (but also with the highest computational cost) is to use method 1 with B3LYP/6-31+G* in combination with the solvent model (R^2 = 0.997). The fact that both correlation methods lead to linear relationships might stem from a linear dependence of the relaxation energy for radical cations $\mathbf{2}^{\bullet+}$.

To expand the oxidation potential of system **2** farther into the positive range, the introduction of moieties with stronger electron-withdrawing character is necessary. In Table 3, the predicted oxidation potentials of three conceivable nitro-substituted derivatives (**2i**−**2k**) are summarized. To obtain this information, the approach involving I_P* (calculation method 1, B3LYP/6-31G*, vacuum) was used. The results suggest that the present limit of 1.09 V versus Ag/$AgNO_3$ (**2h**)

Table 2. Intercepts, Slopes, and Coefficients of Determination (R^2) for Linear Regressions of the Plots of $E_{ox,1}$ versus Calculated I_P and ε_H, Respectively

level of theory	method 1 (I_p*)			method 2 (ε_H)		
	intercept	slope	R^2	intercept	slope	R^2
B3LYP/6-31G* (vac.)	−2.619	0.553	0.982	−2.054	−0.569	0.939
B3LYP/6-31+G* (vac.)	−2.864	0.570	0.986	−2.339	−0.592	0.956
B3LYP/6-31+G* (CH_3CN)	−3.509	0.856	0.997	−3.732	−0.846	0.993

Table 3. Projection of the Oxidation Potentials $E_{ox,1}$ (vs Ag/$AgNO_3$) of Nitro-Substituted Phenanthroimidazoles 2i−2k Using Calculation Method 1 (B3LYP/6-31G*, vacuum)

no.	R^1	R^2	I_P* (eV)	$E_{ox,1}$ (V)
2i	H	NO_2	6.87	1.18
2j	NO_2	H	7.34	1.44
2k	NO_2	NO_2	7.70	1.64

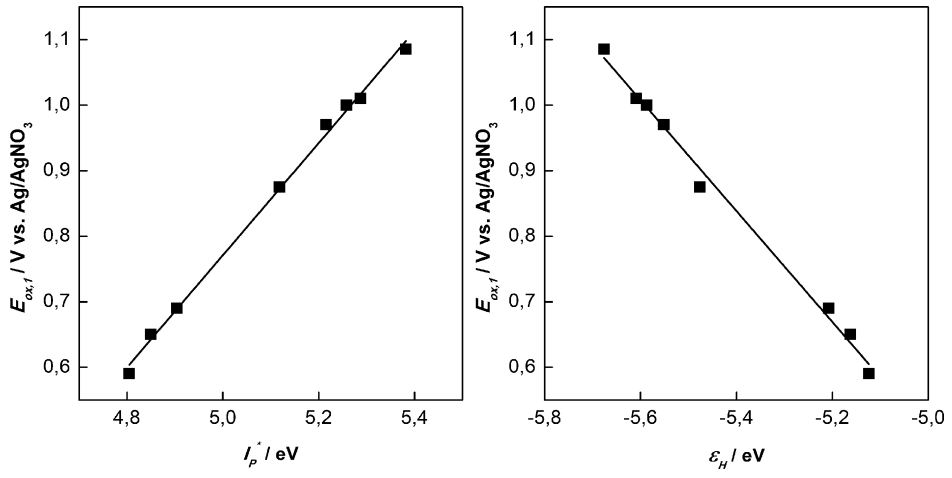

Figure 4. Correlations of $E_{ox,1}$ with I_P* (left) and $E_{ox,1}$ with ε_H (right) for series **2** (I_P* and $E_{ox,1}$ were calculated using B3LYP/6-31+G* and the PCM solvent model).

dx.doi.org/10.1021/ja410865z | J. Am. Chem. Soc. 2014, 136, 427−435

could be steadily increased up to 1.64 V (**2k**) by stepwise introduction of NO_2 groups. This extension would result in a potential range of 1.05 V for compounds **2a**−**2k**. With respect to indirect electro-organic synthesis, the oxidation potentials of most common functional groups would be covered by mediator system **2**.[53] Considering the fact that for a mediated electron transfer the redox potential of the mediator can be up to 0.5 V below the potential of the substrate, this range ought to be even broader.[7,8,28,54]

Application of 2 as Electrocatalyst. To establish that **2** can serve as a useful mediator, we selected two substrates, viz. *p*-anisyl alcohol (**6**) with an oxidation potential of 1.21 V versus $Ag/AgNO_3$ and *p*-anisyl-*n*-octyl ether **7** (E_{ox} = 1.33 V vs $Ag/AgNO_3$). From series **2**, we selected mediators **2c** and **2a** whose oxidation potentials are 1.00 and 1.09 V, respectively (note Table 1). For the oxidation of **6**, mediator **2c** appeared to be a suitable candidate, the potential difference between the two being 0.21 V. For **7**, mediator **2a** was a promising candidate with ΔE_{ox} = 0.24 V. The results of the cyclic voltammetry studies are shown in Figure 5 (the currents are normalized to

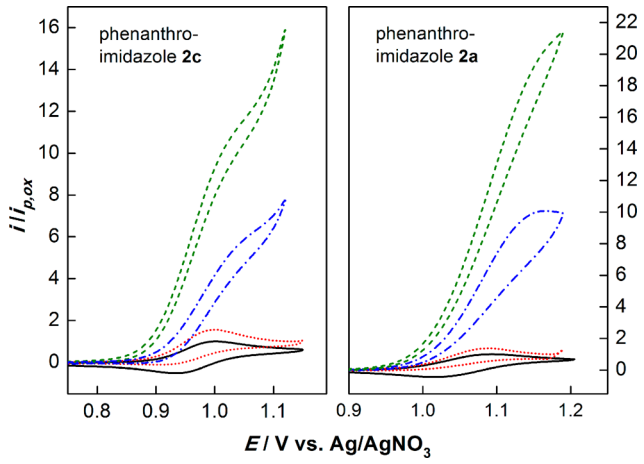

Figure 5. Cyclic voltammograms of mediators **2c** (left) and **2a** (right): black lines, 1 mM **2**; red dotted line, 1 mM **2** + 20 mM substrate; blue dash-dotted line, 1 mM **2** + 20 mM substrate +5 mM 2,6-lutidine; green dashed line, 1 mM **2** + 20 mM substrate + 50 mM 2,6-lutidine; substrates, *p*-anisyl alcohol (**6**; left) and *p*-anisyl-*n*-octyl ether (**7**; right).

the peak current of the mediator). In both cases, addition of 20 mM substrate to the electrolyte containing 1 mM mediator leads to low catalytic currents (compare black line to red dotted line). In addition, oxidation of the mediator becomes irreversible due to the existence of a chemical reaction that serves to drain the initial electron transfer equilibrium process. Assuming that the oxidation pathway illustrated in Scheme 1 is applicable, the addition of a base should facilitate the chemical follow-up reaction. In fact, in a previous study, we have shown that for the oxidation of benzylic substrates with mediators **1** the addition of base is essential; 2,6-lutidine proved to be an excellent choice.[27] In the case of mediators **2**, this also proved to be the case. Upon the addition of 5 mM 2,6-lutidine to mediator **2c** and substrate **6**, the current at the peak potential $E_{ox,1}$ increases by a factor of 4 compared to the peak current in the absence of substrate and base (by a factor of 6 in the case of **2a**/**7**, see blue dash-dotted lines). The catalytic current is clearly dependent on the concentration of the base because increasing the concentration of lutidine to 50 mM led to an increase by a factor of 9 for **2c**/**6** and by a factor of 12 in the case of **2a**/**7** (green dashed lines). It was also confirmed that this increase of the current does not stem from a potential shift of the oxidation potential of the substrate upon addition of base (see Figure S7). It should be noted that the catalytic currents of mediators **2a** and **2c** are much more pronounced compared to the electro-oxidation of **6** and **7** using triarylimidazole catalysts **1a** and **1c** under the same conditions (see Figures S8 and S9). With a base concentration of 50 mM, the current at the mediator peak potential is increased by a factor of 2 to 4.

A potentiostatic bulk electrolysis was conducted at 0.98 V versus $Ag/AgNO_3$, using mediator **2a** in combination with substrate **6** in a divided cell (experimental details; see Supporting Information). The oxidation product *p*-anisaldehyde was obtained in a 75% isolated yield (95% with respect to recovered starting material). The cyclic voltammetry data and the product selectivity suggest that the reaction mechanism in Scheme 1 (right side) is also applicable for this case.

CONCLUSION

Using our generalized synthetic procedure, substituted phenanthroimidazoles **2** are easy to synthesize. With the derivatives prepared so far, an oxidation potential range of 0.5 V is accessible, which is wide enough to oxidize many common functional groups, especially when it is taken into account that for a mediated electron transfer the redox potential of the mediator can be up to 0.5 V below the potential of the substrate, sometimes more.[7,8,28,54]

In comparison to the triarylimidazoles **1**, the influence of the aryl substituents on the first oxidation event is dramatically increased, and their redox behavior is far more reversible. Since the phenanthroimidazole framework provides an opportunity for tuning the redox potential (two different types of substituents in the *para* position can be introduced in one step), the potential range could be extended beyond that we have explored thus far by using substituents with stronger electron-donating or electron-withdrawing properties, such as amino or nitro groups.

With the calculation of I_p* and ε_H and the correlation to $E_{ox,1}$ of a set of derivatives, we are able to predict the oxidation potentials of phenanthroimidazoles not yet synthesized. Consequently, tedious trial-and-error synthesis in order to obtain a system with the desired oxidation potential can be avoided. Furthermore, the level of accuracy can be adjusted to fit the problem. Very precise values (R^2 = 0.997) can be obtained by calculating I_p* but at the expense of extended computation times (B3LYP/6-31+G* and solvent model). A rapid estimation can be accomplished with lower accuracy by simply determining $\sum\sigma^+$ (R^2 = 0.969) or ε_H (R^2 = 0.939 using B3LYP/6-31G* in vacuum). The application of these prediction methods suggests that the potential range can be extended to 1.05 V by introducing nitro groups.

Finally, by using simple model substrates, we have demonstrated that **2** can be applied as mediator in indirect electro-organic synthesis. In future studies, we intend to explore the substrate spectrum for this promising new class of mediators and to expand the potential range by synthesis of new phenanthroimidazole derivatives.

ASSOCIATED CONTENT

Supporting Information

Detailed synthetic procedures, spectral data, description of the electrochemical methods, supporting figures, computational

dx.doi.org/10.1021/ja410865z | J. Am. Chem. Soc. 2014, 136, 427−435

parameters. This material is available free of charge via the Internet at http://pubs.acs.org.

AUTHOR INFORMATION

Corresponding Author

little@chem.ucsb.edu

Notes

The authors declare no competing financial interest.

ACKNOWLEDGMENTS

We acknowledge partial support from the Center for the Sustainable Use of Renewable Feedstocks (CenSURF), an NSF Center for Chemical Innovation (CHE-1240194). R.F. is particularly grateful to the Alexander von Humboldt Foundation for granting a Feodor Lynen Fellowship. We are pleased to acknowledge the contributions of Professor Dean Tantillo (University of California, Davis, CA) to our initial application of quantum calculations to the present problem.

REFERENCES

(1) Frontana-Uribe, B. A.; Little, R. D.; Ibanez, J. G.; Palma, A.; Vasquez-Medrano, R. *Green Chem.* **2010**, *12*, 2099−2119.
(2) Schäfer, H. J.; Harenbrock, M.; Klocke, E.; Plate, M.; Weiper-Idelmann, A. *Pure Appl. Chem.* **2007**, *79*, 2047−2057.
(3) Sperry, J. B.; Wright, D. L. *Chem. Soc. Rev.* **2006**, *35*, 605.
(4) Utley, J. H. P.; Folmer Nielsen, M. Electrogenerated Bases. In *Organic Electrochemistry*, 4th ed.; Lund, H., Hammerich, O., Eds.; M. Dekker: New York, 2001; pp 1227−1258.
(5) Moeller, K. D. *Tetrahedron* **2000**, *56*, 9527−9554.
(6) Savéant, J.-M. *Chem. Rev.* **2008**, *108*, 2348−2378.
(7) Steckhan, E. *Top. Curr. Chem.* **1987**, *142*, 1−69.
(8) Steckhan, E. *Angew. Chem., Int. Ed. Engl.* **1986**, *25*, 683−701.
(9) Simonet, J.; Pilard, J.-F. Electrogenerated Reagents. In *Organic Electrochemistry*, 4th ed.; Lund, H., Hammerich, O., Eds.; M. Dekker: New York, 2001; pp 1163−1225.
(10) Platen, M.; Steckhan, E. *Chem. Ber.* **1984**, *117*, 1679−1694.
(11) Saito, K.; Ueoka, K.; Matsumoto, K.; Suga, S.; Nokami, T.; Yoshida, J.-I. *Angew. Chem., Int. Ed.* **2011**, *50*, 5153−5156.
(12) Hosoi, K.; Inagi, S.; Kubo, T.; Fuchigami, T. *Chem. Commun.* **2011**, *47*, 8632−8634.
(13) Park, Y. S.; Little, R. D. *Electrochim. Acta* **2009**, *54*, 5077−5082.
(14) Park, Y. S.; Little, R. D. *J. Org. Chem.* **2008**, *73*, 6807−6815.
(15) Park, Y. S.; Wang, S. C.; Tantillo, D. J.; Little, R. D. *J. Org. Chem.* **2007**, *72*, 4351−4357.
(16) Gerken, J. B.; Wang, S. C.; Preciado, A. B.; Park, Y. S.; Nishiguchi, G.; Tantillo, D. J.; Little, R. D. *J. Org. Chem.* **2005**, *70*, 4598−4608 and references cited therein.
(17) König, B., Ed. *Chemical Photocatalysis*; De Gruyter: Berlin, 2013.
(18) Xu, K. *Chem. Rev.* **2004**, *104*, 4303−4418.
(19) Takahashi, K.; Furusawa, T.; Sawamura, T.; Kuribayashi, S.; Inagi, S.; Fuchigami, T. *Electrochim. Acta* **2012**, *77*, 47−53.
(20) Halas, S. M.; Okyne, K.; Fry, A. J. *Electrochim. Acta* **2003**, *48*, 1837−1844.
(21) Fuchigami, T.; Tetsu, M.; Tajima, T.; Ishii, H. *Synlett* **2001**, 1269−1271.
(22) Wend, R.; Steckhan, E. *Electrochim. Acta* **1997**, *42*, 2027−2039.
(23) Dapperheld, S.; Steckhan, E.; Brinkhaus, K. H. G.; Esch, T. *Chem. Ber.* **1991**, *124*, 2557−2567.
(24) Schmidt, W.; Steckhan, E. *Chem. Ber.* **1980**, *113*, 577−585.
(25) Yurchenko, O.; Freytag, D.; Zur Borg, L.; Zentel, R.; Heinze, J.; Ludwigs, S. *J. Phys. Chem. B* **2012**, *116*, 30−39.
(26) Seo, E. T.; Nelson, R. F.; Fritsch, J. M.; Marcoux, L. S.; Leedy, D. W.; Adams, R. N. *J. Am. Chem. Soc.* **1966**, *88*, 3498−3503.
(27) Zeng, C.-C.; Zhang, N.-T.; Lam, C. M.; Little, R. D. *Org. Lett.* **2012**, *14*, 1314−1317.
(28) Zhang, N.-T.; Zeng, C.-C.; Lam, C. M.; Gbur, R. K.; Little, R. D. *J. Org. Chem.* **2013**, *78*, 2104−2110.
(29) Kwon, J. E.; Park, S.; Park, S. Y. *J. Am. Chem. Soc.* **2013**, *135*, 11239−11246.
(30) Mao, M.; Wang, J.-B.; Xiao, Z.-F.; Dai, S.-Y.; Song, Q.-H. *Dyes Pigm.* **2012**, *94*, 224−232.
(31) Wang, Z.; Lu, P.; Chen, S.; Gao, Z.; Shen, F.; Zhang, W.; Xu, Y.; Kwok, H. S.; Ma, Y. *J. Mater. Chem.* **2011**, *21*, 5451.
(32) Yuan, Y.; Li, D.; Zhang, X.; Zhao, X.; Liu, Y.; Zhang, J.; Wang, Y. *New J. Chem.* **2011**, *35*, 1534.
(33) Park, S.; Kwon, J. E.; Kim, S. H.; Seo, J.; Chung, K.; Park, S.-Y.; Jang, D.-J.; Medina, B. M.; Gierschner, J.; Park, S. Y. *J. Am. Chem. Soc.* **2009**, *131*, 14043−14049.
(34) Compound **2b** has been reported before: Nielsen, C. B.; Pittelkow, M.; Sørensen, H. O. *Acta Crystallogr. E* **2005**, *61*, 955−956. However, NMR and MS data have not been published to date.
(35) Boden, B. N.; Jardine, K. J.; Leung, A. C. W.; MacLachlan, M. J. *Org. Lett.* **2006**, *8*, 1855−1858.
(36) Brunner, K.; van Dijken, A.; Börner, H.; Bastiaansen, J. A. M.; Kiggen, N. M. M.; Langeveld, B. M. W. *J. Am. Chem. Soc.* **2004**, *126*, 6035−6042.
(37) Karimi-Jaberi, Z.; Barekat, M. *Chin. Chem. Lett.* **2010**, *21*, 1183−1186.
(38) Steck, E. A.; Day, A. R. *J. Am. Chem. Soc.* **1943**, *65*, 452−456.
(39) The fact that 1*H*-phenanthroimidazoles are easily alkylated at position 1 might prove useful in other regards. For instance, position 1 could serve as a linking site for modification of an electrode surface with **2** serving as heterogeneous catalyst.
(40) Pavlishchuk, V. V.; Addison, A. W. *Inorg. Chim. Acta* **2000**, *298*, 97−102.
(41) Bard, A. J.; Faulkner, L. R. *Electrochemical Methods: Fundamentals and Applications*; Wiley: New York, 2001.
(42) Zuman, P. *Substituent Effects in Organic Polarography*; Plenum Press: New York, 1967.
(43) Hicks, L. D.; Fry, A. J.; Kurzweil, V. C. *Electrochim. Acta* **2004**, *50*, 1039−1047.
(44) Wu, X.; Davis, A. P.; Lambert, P. C.; Kraig Steffen, L.; Toy, O.; Fry, A. J. *Tetrahedron* **2009**, *65*, 2408−2414.
(45) The Gaussian '09 package was used for the calculations: Frisch, M. J.; Trucks, G. W.; Schlegel, H. B.; Scuseria, G. E.; Robb, M. A.; Cheeseman, J. R.; Scalmani, G.; Barone, V.; Mennucci, B.; Petersson, G. A.; Nakatsuji, H.; Caricato, M.; Li, X.; Hratchian, H. P.; Izmaylov, A. F.; Bloino, J.; Zheng, G.; Sonnenberg, J. L.; Hada, M.; Ehara, M.; Toyota, K.; Fukuda, R.; Hasegawa, J.; Ishida, M.; Nakajima, T.; Honda, Y.; Kitao, O.; Nakai, H.; Vreven, T.; Montgomery, J. A., Jr.; Peralta, J. E.; Ogliaro, F.; Bearpark, M.; Heyd, J. J.; Brothers, E.; Kudin, K. N.; Staroverov, V. N.; Kobayashi, R.; Normand, J.; Raghavachari, K.; Rendell, A.; Burant, J. C.; Iyengar, S. S.; Tomasi, J.; Cossi, M.; Rega, N.; Millam, N. J.; Klene, M.; Knox, J. E.; Cross, J. B.; Bakken, V.; Adamo, C.; Jaramillo, J.; Gomperts, R.; Stratmann, R. E.; Yazyev, O.; Austin, A. J.; Cammi, R.; Pomelli, C.; Ochterski, J. W.; Martin, R. L.; Morokuma, K.; Zakrzewski, V. G.; Voth, G. A.; Salvador, P.; Dannenberg, J. J.; Dapprich, S.; Daniels, A. D.; Farkas, Ö.; Foresman, J. B.; Ortiz, J. V.; Cioslowski, J.; Fox, D. J. *Gaussian 09*, revision D.01; Gaussian, Inc.: Wallingford, CT, 2009.
(46) Marenich, A. V.; Cramer, C. J.; Truhlar, D. G. *J. Phys. Chem. B* **2009**, *113*, 6378−6396.
(47) Hubig, S. M; Rathore, R.; Kochi, J. K. *J. Am. Chem. Soc.* **1999**, *121*, 617−626.
(48) Due to the low solubility of mediators **2a** and **2b** in acetonitrile, the addition of dichloromethane was required (CH_3CN/CH_2Cl_2 = 4:1). Since the oxidation potentials of **2c**−**2h** do not change significantly upon the addition of dichloromethane to the acetonitrile solution, we are confident that our approach is still valid.
(49) Szabo, A.; Ostlund, N. S. *Modern Quantum Chemistry*; Dover Publications: Mineola, NY, 1996.
(50) Perdew, J.; Levy, M. *Phys. Rev. B* **1997**, *56*, 16021−16028.
(51) Chong, D. P.; Gritsenko, O. V; Baerends, E. J. *J. Chem. Phys.* **2002**, *116*, 1760−1772.
(52) In contrast to the Hammett plots, the intercepts of the linear fits in Figure 4 have no specific physical meaning other than the oxidation

potential of a hypothetical compound with either equal energy of neutral and charged form (for $E_{ox,1}$ vs I_P*) or with an ε_H on the vacuum level (for $E_{ox,1}$ vs ε_H). Interestingly, for both methods, the absolute value of the slope is between 0.55 and 0.59 for the vacuum calculation and around 0.85 for the solvent-corrected method. Ideally, a slope of unity would be obtained in a plot of electronvolts versus volts. Deviations might stem from solvation effects, which is in agreement with the slope closer to unity when the solvent model is used. A more detailed discussion can be found in Davis, A.; Fry, A. J. *J. Phys. Chem. A* **2010**, *114*, 12299−12304.

(53) Weinberg, N. L.; Weinberg, H. R. *Chem. Rev.* **1968**, *68*, 449−523.

(54) Miranda, J. A.; Wade, C. J.; Little, R. D. *J. Org. Chem.* **2005**, *70*, 8017−8026.